

Acoustic Metamaterial for Image Detection

Siti Zaleha Abdul Hamid^{1*}, Nur Farah Hanis Dau¹d, Herlina Abdul Rahim¹, Ruzairi Abdul Rahim^{2,1}

¹Faculty of Electrical Engineering, Universiti Teknologi Malaysia, 81310 Skudai, Johor, Malaysia

² Faculty of Electrical Engineering, Universiti Teknologi Malaysia, 81310 Skudai, Johor, Malaysia

²Faculty of Electrical & Electronic Univeriti Tun Hussein Onn Malaysia.

Abstract

Image detection is important especially in medical for non destructive examination. Early development of image detection used high frequency for clearer image and caused heat development. Hence, there is a need to design metamaterial that can detect the image with lower frequency. This study focused on hole structured of three dimensions (3D) metamaterial. Methodology for this study can be divided into three parts which are metamaterial design, metamaterial testing, and performance analysis. The hole size, type of material and thickness of metamaterial designed will be varied for performance comparison. The image produce at the output plane of the metamaterial is clearly with the smallest scale size of hole which is 1.5 mm and the thickness of the metamaterial at 130 mm is equal with the operating wavelength. The device perfectly operated at lower frequency of 2.6 kHz.

Keywords: Metamaterial, Image Detection, Acoustic Metamaterial.

1. Introduction

Image detection is one of the important tools in image processing that applied in several areas of science and technology especially in medical for non-destructive testing through computer vision imaging device. For instance, ultrasound frequency is used in medical imaging device to see internal organ and body structure and find source of disease. Ultrasound used high frequency (range higher than 20 kHz) and has drawback to patient who had frequent examinations by using ultrasound probe [1] as the absorption of ultrasound energy by tissue or water cause heat development [2]. Meanwhile, the local heat from the ultrasound causes formation of bubble due to dissolves gases. However, high frequency of ultrasound is required in producing clearer image [3].

*corresponding author: szaleha@utm.my

Acoustical imaging by acoustic microscopy used a high frequency ultrasound range from five MHz to three GHz. The purposed acoustic microscopy was to produce magnified view of structures [7]. The earlier development of operational acoustic microscopy focused on the visualization method of low frequency ultrasonic, adaptation of high frequency [8] [9].

The maximum achievable resolution of any imaging device is limited by the wavelength of the used radiation (diffraction limit) [4]. The image of an object is clarified by evanescent waves that scattered from the object due to the formation of Fabry-Perot transmission resonances. A device capable creating image with only evanescent waves would generate only the significant information contained in image that is the shape of an object. The evanescent wave has several ways to overcome the diffraction limit of classical wave such as light or sound. The previous study proved that diffraction limit can be overcome by superlenses [5] and time reversal techniques [6]. Moreover, these approach able to restore evanescent wave and provide the details of an object on its image.

Recently, various study on metamaterial performed in acoustic to control and manipulate the physic properties of sound waves. Acoustic metamaterial shows it ability to restore the propagative and evanescent waves and produce subwavelength imaging. This capability of matematerial had shown the possibility of overcoming the diffraction limit. Hence, there is a need to design metamaterial that can act as nearly imaging device, detect the image with lower frequency, and provide new acoustical properties in term of sound propagation. This study focused on holey structured of metamaterial. The size of hole, type of material and thickness of metamaterial designed will be varied for performance comparison. The holey structure of 3 dimension (3D) metamaterial transmits evanescent field components of object efficiently due to the formation of Fabry- Parot inside the holey structure and detect the image with lower frequency by placing the object between the sound source and metamaterial.

1.1 Acoustic Metamaterial

Metamaterial is manmade structure to have a property that cannot be found in nature, which arranged in repeating pattern and provide the less scale than wavelength of phenomenon they influence. By having these smart properties, they are able to manipulate the electromagnetic waves by blocking, absorbing, enhancing, and bending wave to achieve better performance that go beyond the limit of conventional materials [16].

1.2 Acoustic Microscopy

The working principle of scanning acoustic microscopy is as shown in Figure 1.1. The transducer converts the electrical impulse that provided by the pulser into the ultrasonic signal. A very fast switch swaps several thousand times a second between sending and receiving state. The transducer receives the echoes reflected by sample layers. The ultrasonic signal is converted back to an electrical pulse by transducer. Time of flight, amplitude and phase of the pulse is analyzed. The extracted information is transcript into a grey scale picture [10].

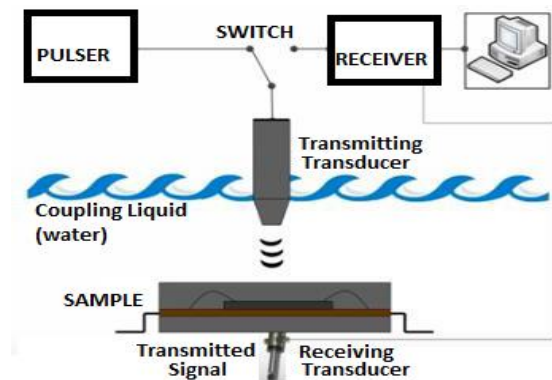


Figure 1.1 Working Principle Pulse Echo Modes

In transmission mode, the receiving transducer underneath the sample picks up the transmitted part of the ultrasonic signal. A flat and even is the ideal case for ultrasonic inspections. The sound waves are able to couple into the sample very well over the full area. It is possible to investigate curved samples but only under certain conditions. Special customized hardware is necessary. Meanwhile sample with a rough and bumpy surface can be investigated dependent on the degree of roughness and the used frequency.

Pulse echo have different transmission mode, which are A-mode, B-mode, C-mode, and M-mode. This study performed in C-mode for three dimension (3D) image. In this mode, 'C' stands for constant depth. It is basic electronic gate a portion of A-scan signal is used to brightness modulate the display of a plane t a specific depth from the transducer plane (tomograph). The applications are 3D ultrasound, peripheral IV access and handhelds.

1.3 The Effect on Snell's Law

The basis of permeability, μ and permittivity, ϵ can classify the material into first quadrant ($\mu>0, \epsilon>0$), second quadrant ($\epsilon<0, \mu>0$), third quadrant ($\epsilon<0, \mu<0$), and fourth quadrant ($\epsilon>0, \mu<0$) (Anantha S. & Ramakrishna, 2013). The third quadrant shows metamaterial properties as double negative material. The propagation waves follow the left hand rule. The refractive index of the medium became negative as both permittivity and permeability are in negative region.

Figure 1.2 shows the Snell's law in different medium. Negative refractive index in the third quadrant is the effect of Snell's law when the negative refraction occurred at incident wave at interface ray that bend inside in DNG medium while the transmitted wave in DPS medium is opposing to positive index after refracted at the interface Ray bends inside.

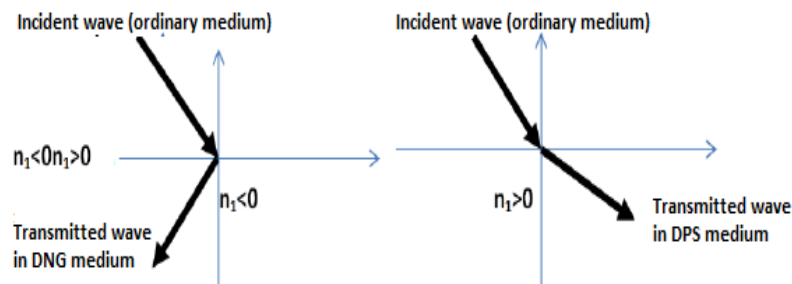


Figure 1.2 Snell's Law in Difference Medium

1.4 Related Study on Acoustic Metamaterial

There are several application of metamaterial such as antenna [18], sensor [20], and superlens [19]. Metamaterial helps antenna gives small wavelength, which is one fifth of operating wavelength [18], improves the sensitivity and the resolution of sensors by special properties [20], and make superlens capables to clear of the diffraction limit [19].

In acoustic imaging, recent studies discussed that acoustic superlenses or magnified hyperlenses resolve the diffraction limit of conventional imaging device by converting the evanescent wave of the acoustic hyperlens to propagating wave and significantly magnified the subwavelength of the object. Evanescent wave needed to overcome diffraction limit in order to provide detail image. A study had demonstrated that the fabricated acoustic hyperlens relies on straightforward cut-off free propagation and achieve deep subwavelength resolution with low loss over a broad frequency bandwidth [13]. Another studies pointed out that metamaterial hyperlens could overcome diffraction limit by providing smaller than a half

of the operating wavelength. The capability of the device not only transmits information carried by evanescent wave, but also magnified it as the information travels to the far-field outside the lens [14] [15].

1.5 Acoustic Metamaterial Design

Several studies of metamaterial had reported several metamaterial design based on their theories and applications [21] [22] [23]. Normally, researchers designed the material by arranging the structure in periodic pattern with a scale that much smaller than their operating wavelength. Previously, [23] had designed 36 brass fins (long: 20cm, thickness: 3mm, inner radiu: 2.7mm, outer radius: 21.8cm) applied with frequency range of 4.2 to 7 kHz to study the potential of acoustic hyperlens in sharpening the ultrasound image. Then, double negative acoustic metamaterial was studied by [21] using a designed with plastic metamaterial (length: 29mm, inner diameter: 7mm, and outer diameter: 1mm) at frequency range of 5.38 to 5.94 kHz. Others, holey structure brass alloy matamaterial (square hole: 40x40, hole size: 0.79mm, height: 158mm, wall thickness: 0.79mm) was designed by [22] for an acoustic deep-subwavelength imaging at frequency of 2.18 kHz.

Metamaterial are normally designed and fabricated by arranged a structure of unit cells in repeated pattern. The periodic structure is used to implement the metamaterial. From literature, brass alloy metamaterial designed with perforate structure in repeated pattern successfully transferred information carried by evanescent wave through the metamaterial at the lowest frequency.

1.6 Fabry-Perot Resonance Inside Holey Structure of Metamaterial

Fabry-Perot as shown in Figure 1.3 is happened when incoming wave is repeatedly refracted and reflected between the two surface of wall inside the hole produce multiple beam that are then focused together, causing self-interference of wave [24].

This phenomenon take place in transmission when there is zero order transmission coefficients, t for an acoustic wave with parallel momentum, $b_{\parallel} = (b_x^2 + b_y^2)^{1/2}$ can be defined as equation 1.1 where the propagation constant, $q_z = k_0 = 2\pi/\lambda$ and waveguide mode, $S_{00} = a/\lambda$ and $Y = b_0/(b_0^2 + b_{\parallel}^2)^{1/2}$.

$$t(\lambda, b_{\parallel}) = \frac{4|S_{00}|^2 Y \exp(iqh)}{(1 + Y|S_{00}|^2)^2 - (1 - Y|S_{00}|^2)^2 \exp(2iq_z h)} \quad (1.1)$$

This theory suggested that if an object is placed in front of the metamaterial, the image of the object is transferred through the holey plate and formed at the output of the metamaterial [25].

The parallel momentum is not affected by the dispersion inside the hole, so $\rho_{effz} = 1 / \beta_{effz} = \infty$. While for x and y direction, the metamaterial is defined as equal density, which is, $\rho_{effx} = \rho_{effy} = \rho_{eff} = \rho_{air} \beta^2 / a^2$ and bulk modulus, $K_{effx} = K_{effy} = K_{eff} = K_{air} \beta^2 / a^2$ and the velocity of sound is considered equal to air.

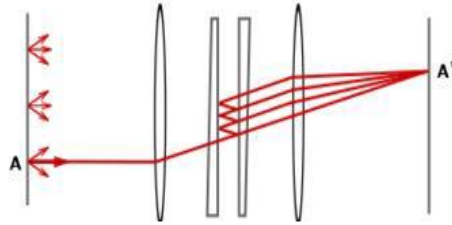


Figure 1.3 Formation of Fabry-Perot

2. Methodology

Methodology for this study can be divided into three parts which are metamaterial design, metamaterial testing, and performance analysis.

2.1 Metamaterial Design

The metamaterial was designed with perforate structure in repeated pattern as shown in Figure 1.4. The holey structure of metamaterial consisted of holes arranged in periodic pattern and filled with air. The separation between holes to hole is β for horizontal and vertical line where the size of each hole is a and the height is known as h . The type of material used as the wall for the holes is brass alloy. Hence, the geometrical parameter in the experimental was chosen are $a = 1.5\text{mm}$, $\beta = 3\text{mm}$, $h = 130\text{mm}$ and number of holes = 100 (10x10).

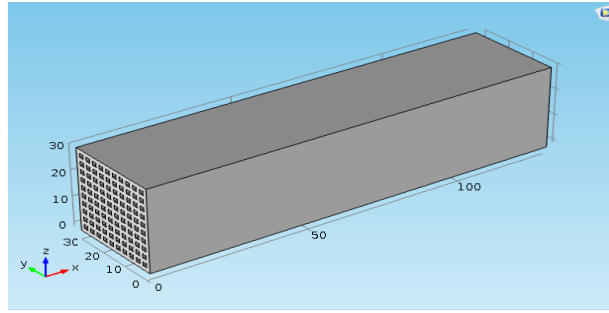


Figure 1.4 The Holey Structure of Metamaterial

2.2 Metamaterial Testing

Then, the metamaterial designed (the holey structure) was tested in COMSOL Multiphysics to observe the response of the designed and further justify the results obtained. In COMSOL, the metamaterial was designed in 3D with physical properties and position set as in the real experiment by using acoustic pressure with frequency domain. Frequency range used is from 5 Hz to 3 kHz and the type of material is alloy (UNS C26000) with density 8530 kgm^3 . The speed of sound for the sound propagation from the source is 343 ms^{-1} . The experiment was conducted in air where the most front of boundary was set as sound source with initial pressure 20 Pa. The metamaterial was set 20 cm from the source and the object was set 3 mm from the input of metamaterial. The other end of the metamaterial is the output region where the image of the object formed. The experimental arrangement in COMSOL is as shown in Figure 1.5.

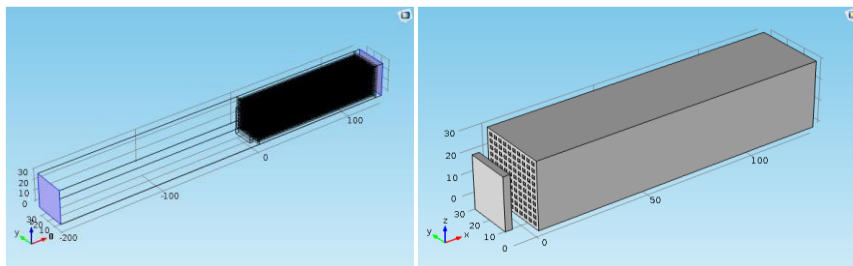


Figure 1.5 Experimental Diagrams in COMSOL

Three models constructed with different variable parameters were simulated in COMSOL for performance comparison. The simulation were performed with ideal design first before repeated by varying the square size of the hole, a by varying the thickness of the metamaterial, h and by replacing the holey plate with square long wire as in electromagnetic case. The result of pressure distribution at the output side for each model was observed.

2.3 Performance Analysis

The performance of design is measured based on the capability to meet the requirement of metamaterial design where the operation wavelength obtained must be approximate to the metamaterial thickness ($\lambda \approx h$), much more than hole size ($\lambda \gg a$) and much more than the separation between hole to hole ($\lambda \gg \beta$) [22]. The operating wavelength, λ can be calculated as equation 1.2 where c is speed of sound ($c=343 \text{ ms}^{-1}$) and f is the operating frequency (kHz).

$$\lambda = c/f \quad (1.2)$$

3. Results and Discussions

The simulation test result shows in Figure 1.6 is the image of the rectangular object that was placed in front of the metamaterial for ideal design with hole size, a of 1.5 mm and metamaterial thickness, h of 130 mm.

The graph in Figure 1.7 portray that the highest pressure distribution inside the structure metamaterial was at frequency of 2.6kHz. From this graph, horizontal axis represents the position of the arrangement of the experimental simulation where at 0 mm was the incident plane wave and 200 mm was the position of metamaterial (metamaterial was placed 20 cm away from the source).

The operation wavelength was calculated as equation 1.2. From Table 1.2, this ideal design work at frequency, f of 2.6 kHz with operational wavelength, λ of 130 mm and meet the requirement of metamaterial design where ($\lambda \approx h$) and ($\lambda \gg a, \beta$) [22].

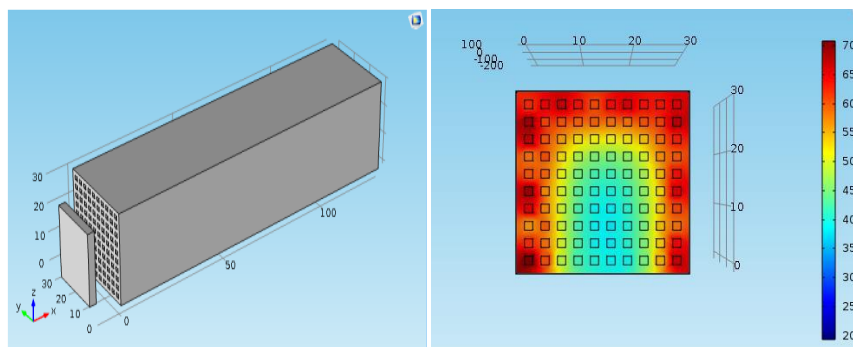


Figure 1.6 Figures of Input Object and Image at Output Plane

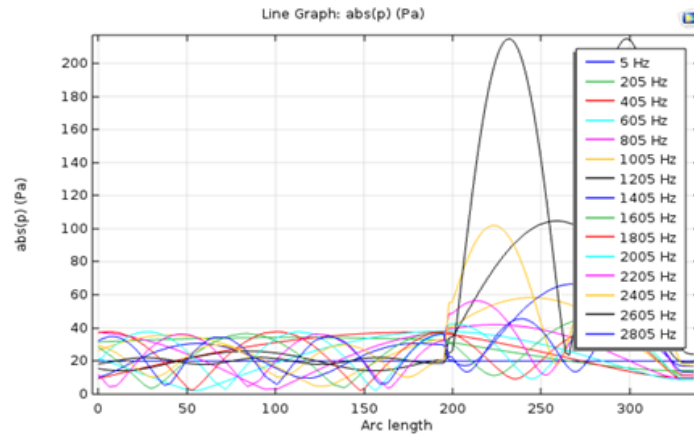


Figure 1.7 Graph of Sound Pressure Level at Different Frequency

Table 1.2 COMSOL Simulation Result for Ideal Design

Parameter	Scale
Hole size, a	1.5 mm
Separation between hole to hole, β	3 mm
Metamaterial thickness, h	130 mm
Operating frequency, f	2.6 kHz
Operating wavelength, λ	131 mm

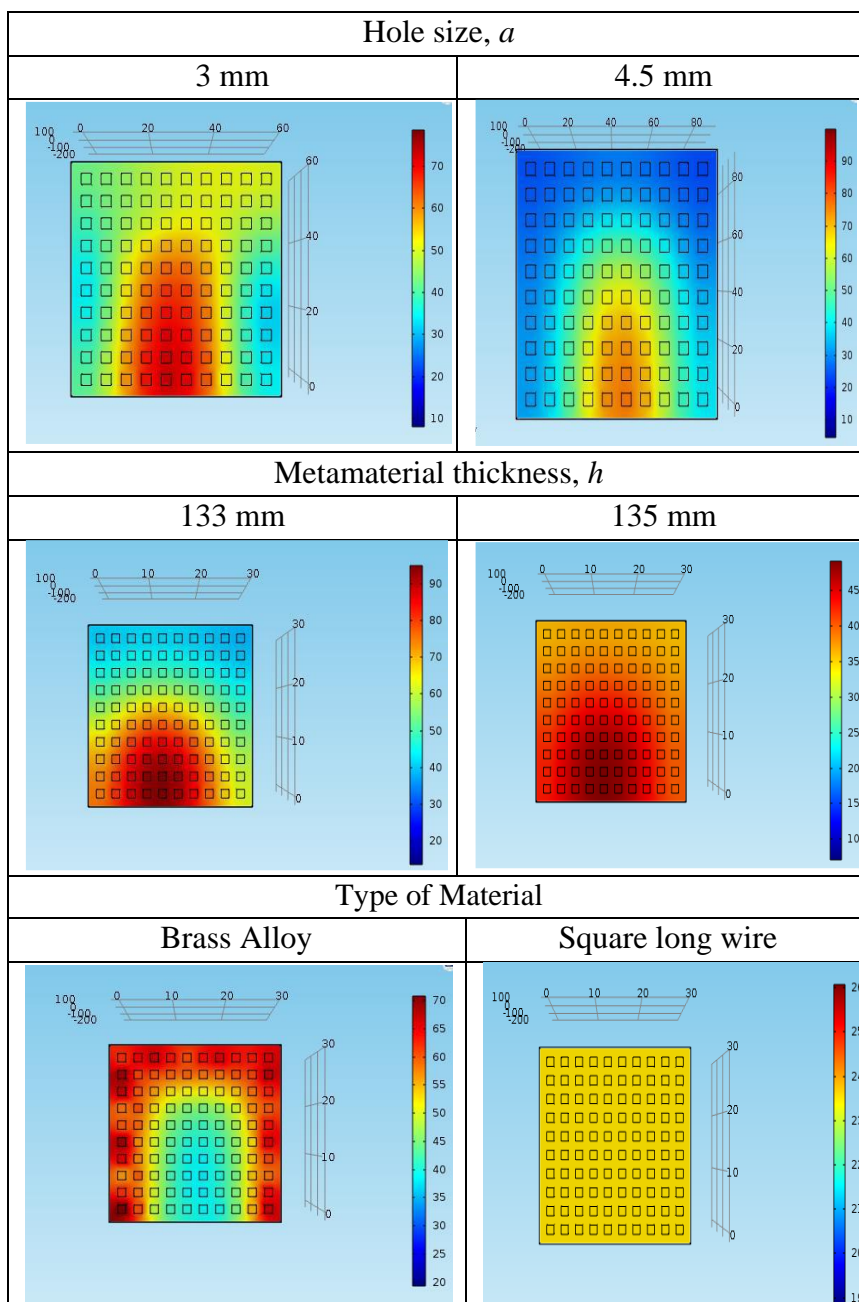
As the image of input object was formed at the output plane, it strongly agreed that the evanescent component of the input object is perfectly transmitted through the metamaterial structure because of formation Fabry-Perot resonance inside the holes [24]. The transmission information through the holey structure is dominated by significant mode propagation and the diffraction effect is neglected because of the operating wavelength is much more larger than the hole size and thickness of wall ($\lambda \gg \beta, a$) [22].

3.1 Performance Comparison

Performance of the metamaterial design were compare by varied the hole size, metamaterial thickness and types of material as tabulated in Table 1.3. From the tabulated data, it can be pointed out that the image of the object at the output plane is become more blurring when the size of hole become larger. Previous research also had discussed about the capability of metamaterial to provide detail and clear image by using the smallest scale of hole as long as less than 1 mm [22]. However, in this study, size of hole could not be less than 1.5 mm due to the lack of memory to simulate smallest scale in COMSOL Multiphysics.

When metamaterial thickness is varied, the image for input object cannot be seen when the thickness of plate, h is more than the operating wavelength, λ . This is because the size does not meet the requirement $\lambda=h$. Meanwhile, the result from the electromagnetic portrayed that there is no image can be formed at the output of metamaterial. The square of wire array do not formed the Fabry-Perot inside the structure because there is difference propagation through structure between acoustic wave and electromagnetic and it is not possible the multiple scattering event in electromagnetic case. This results clearly shown that the periodic array of long wire could not transfer the information from input to output.

Table 1.3 Performance of Metamaterial Design



3.2 Model Performance Tested Without Metamaterial

The simulation result for testing without metamaterial and the graph of pressure distribution for this case are as shown in Figure 1.8 and Figure 1.9 respectively.

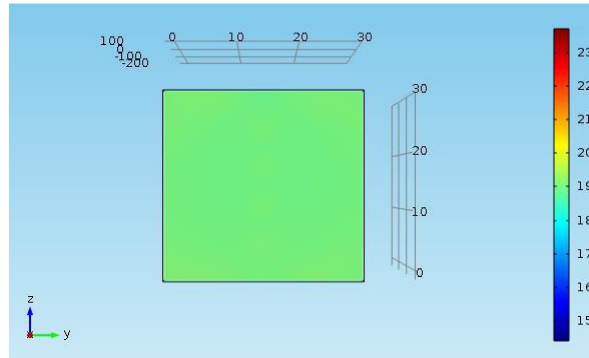


Figure 1.8 Result at the Output Plane Without Metamaterial

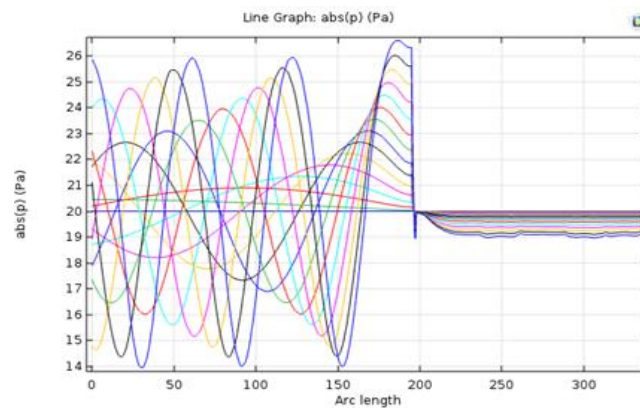


Figure 1.9 Graph of Sound Pressure Level at Different Frequency

Based on the graph shown in Figure 1.9, the sound pressure level become decrease with distance and after the wave propagate beyond the object. There is no image can be seen at the output plane as the object information carried by the wave could not be enhanced without metamaterial.

4. Conclusion and Recommendation

This study proves that an acoustic imaging can be determine by designing and structuring a material with holey metal arranged in periodic pattern at scale that much smaller than the operating wavelength. As a result, the image produce at the output plane of the metamaterial is clearly with the smallest scale size of hole which is 1.5 mm and the thickness of the

metamaterial at 130 mm is equal with the operating wavelength. The device perfectly operated at lower frequency of 2.6 kHz. Although soft blurring at the corners of object, the shape of the whole pattern remains formed at the output plane. Hence, this experiment successfully detected the image from the input of the device. The experimental results confirm the feasibility of metamaterial to detect an image by placing the object between the metamaterial and input source and act as nearly imaging device.

For future recommendation, further study with hardware implementation can be done to corroborate the simulation result from this study. This acoustic imaging device is only using low frequency or known as audible frequency. The hardware experimental can be conduct by using a speaker that send out the sound wave toward an object placed in front of the metamaterial, a microphone attached with 3D stepping scanning to scan the pressure distribution at the output and PC Labview to display the image of the input object. The absorbing material should be place at scanning area to avoid from scanning the bypass sound wave direct from the source and affect the result. The 3D metamaterial can be used to improve the technologies nowadays especially in medical applications or crack detection in engineering structures.

Acknowledgment

The author would like to thank the supervisor for this project for the guide and University Teknologi Malaysia (UTM) for providing facilities for this study

References

- [1] Wu J, O. Dandekar, Nazareth D., Lei P., D'Souza W. and R. Shekhar. (2006). *Effect of Ultrasound Probe on Dose Delivery During Real-time Ultrasound-Guided Tumor Tracking*. International Conference of the IEEE Engineering in Medicine and Biology Society (New York), 3799-3802.
- [2] Karaböce B., Çetin E., Durmuş O. and Özdingiş M. (2016). *Investigation of the temperature effect of ultrasound used in cancer therapy*. Medical Technologies National Congress (TIPTEKNO) (Antalya), 1-4.
- [3] Shung K., Kirk. (2009). *High Frequency Ultrasonic Imaging*. Journal of medical ultrasound. IEEE Trans Ultrason Ferroelectr Freq. Control, (61), 1033–104.
- [4] Maslovski S., Alitalo P. and Tretyakov S. (2008). *Subwavelength-resolution imaging device based on frequency scanning*. Asia-Pacific Microw. Theory Tech. 47, 1-4.
- [5] Pendry, J. B. (2000). *Negative refraction makes a perfect lens*. Phys. Rev. Lett. 85, 3966–3969 (2000).
- [6] Lerosey, G., de Rosny, J., Tourin, A. & Fink, M. (2007) *Focusing beyond the diffraction limit with far-field time reversal*. Science 315, 1120–1122.

- [7] Sokolov, S. (1936). *USSR Patent no. 49 .Aug. 31.1936. British Patent no. 477 (139) .1937. and US Patent no. 21 64 125.*
- [8] Havlice, J., Quate, C.F. and Richardson, B. (1968). *Visualization of sound beams in quartz and sapphire near 1 GHz.* IEEE Ultrason. Symp. IEEE Trans. Sonics Ultrason. SU. 1967, 15-68.
- [9] Korpel, A. (1966). *Visualization of the cross section of a sound beam by Bragg diffraction of light.* Appl. Phys. Lett. 9, 425.
- [10] Davide F., Silvia P., Francesco P., Denis E., Imad Abu Rumeileh. (2013). *A Speed of Sound Aberration Correction Algorithm for Curvilinear Ultrasound Transducers in Ultrasound-Based Image-Guided Radiotherapy.* Physics in Medicine and Bio. 58(5), 1341.
- [11] Erikson R., Fry J., and Jones P. (1970). *Ultrasound in medicine-A review.* IEEE Trans. Sonics Ultrason.vol. SU-21, 144-170.
- [12] Havlice J. and Taenzer J. (1979). *Medical ultrasonic imaging. An overview of principles and instrumentation.*Proc. IEEE. 67, 620-641.
- [13] He, Z., Cai, F., Ding, Y. & Liu, Z. (2008). *Subwavelength imaging of acoustic waves by a canalization mechanism in a two-dimensional phononic crystal.* Appl. Phys. Lett. 93, 233-503.
- [14] Li, J., Fok, L., Yin, X., Bartal, G. & Zhang, X. (2009). *Experimental demonstration of an acoustic magnifying hyperlens.* Nat. Mater. 8, 931–934.
- [15] Lu, D. & Liu, Z. (2012). *Hyperlenses and Metalenses for Far-field Super-Resolution Imaging.* Nat. Commun. 3, 1205.
- [16] Shivola A. (1999). *Electromagnetic Mixing Formula Applications.* Electromagnetic Waves Series, 47 IEEE Trans. Antenna Propag.47, 188-187.
- [17] Anantha S., Ramakrishna. (2013). *Physics of Negative Refractive Index Materials.* PIERS Proceedings. 50, 490-495.
- [18] Azim R. and Islam M. (2013). *Compact planar UWB antenna with band notch characteristics for WLAN and ds-ss.* Progress In Electromagnetics Research. 133, 391-406.
- [19] Fang N. and Xiang Z. (2002). *Imaging properties of a metamaterial superlens.* Proceedings of the 2nd IEEE Conference on Nanotechnology. 225-228.
- [20] Schueler M., Mandel C., Puentes M. and Jakoby R. (2012). *Metamaterial Inspired Microwave Sensors.* IEEE Microw. Magazine. 13, 57-68.
- [21] Shilong Z., Huaijun C., Changlin D. and Xiaopeng Z. (2013). *Double-negative Acoustic Metamaterial based on Meta-Molecule.* J. Phys. D. Appl. Phys. 46, 475-105.
- [22] Zhu J. et al. (2011). *A Holey-Structured Metamaterial for Acoustic Deep-Subwavelength Imaging.* Nat. Phys. 7, 52–55.
- [23] Steven C. (2009). *Acoustic Hyperlens Could Sharpen Ultrasound.* Phy. Rev. Lett. 80, 1734-1736.
- [24] Huhse D., Schell M., Utz W., Kaessner J. and Bimberg D. (1995). *Dynamics of single-mode formation in self-seeded Fabry-Perot laser diodes.* IEEE Photonics Technology Letters, 7, 351-353.
- [25] Jung, J., Garcia-Vidal, F. J., Martin-Moreno, L. & Pendry, J. B. (2009). *Holey metal films make perfect endoscopes.* Phys. Rev. B 79, 153407.